④

AD-A197 930

OFFICE OF NAVAL RESEARCH

Contract N00014-87-J-1118

R & T Code 4133016

Technical Report No. 2

The Surface Enhanced Raman Scattering of the Protonated

Forms of DABCO at a Silver Electrode

by

D.A. Guzonas, D.E. Irish, and G.F. Atkinson

Prepared for Publication

in

Langmuir

DTIC

AUG 2 6 1988

D

Guelph-Waterloo Center for Graduate Work in Chemistry
Waterloo, Campus
Department of Chemistry
University of Waterloo
Waterloo, Ontario
Canada, N2L 3G1

August 8, 1988

AD A197 930

REPORT DOCUMENTATION PAGE

1a. REPORT SECURITY CLASSIFICATION Unclassified		1b RESTRICTIVE MARKINGS			
2a. SECURITY CLASSIFICATION AUTHORITY Unclassified		3 DISTRIBUTION/AVAILABILITY OF REPORT Public Release/Unlimited			
2b DECLASSIFICATION/DOWNGRADING SCHEDULE					
4. PERFORMING ORGANIZATION REPORT NUMBER(S) ONR Technical Report #2		5. MONITORING ORGANIZATION REPORT NUMBER(S)			
6a NAME OF PERFORMING ORGANIZATION D. E. Irish University of Waterloo	6b OFFICE SYMBOL (If applicable)	7a NAME OF MONITORING ORGANIZATION Office of Naval Research			
6c. ADDRESS (City, State, and ZIP Code) Department of Chemistry University of Waterloo Waterloo, Ontario Canada N2L 3G1		7b ADDRESS (City, State, and ZIP Code) The Ohio State University, Research Center 1314 Kinnear Road Room 318 Columbus, Ohio, U.S.A. 43212-1194			
8a. NAME OF FUNDING/SPONSORING ORGANIZATION Office of Naval Research	8b. OFFICE SYMBOL (If applicable)	9 PROCUREMENT INSTRUMENT IDENTIFICATION NUMBER N00014-87-J-1118			
8c. ADDRESS (City, State, and ZIP Code) Chemistry Division 800 N Quincy Street Arlington, VA, U.S.A. 22217-5000		10 SOURCE OF FUNDING NUMBERS			
		PROGRAM ELEMENT NO	PROJECT NO	TASK NO	WORK UNIT ACCESSION NO

11 TITLE (Include Security Classification)

The Surface Enhanced Raman Scattering of the Protonated Forms of DABCO at a Silver Electrode

12 PERSONAL AUTHOR(S)
D.A. Guzonas, D.E. Irish, and G.F. Atkinson

13a TYPE OF REPORT Technical	13b TIME COVERED FROM 1/87 TO 08/88	14. DATE OF REPORT (Year, Month, Day) August 8, 1988	15. PAGE COUNT 45

16. SUPPLEMENTARY NOTATION

Submitted to Langmuir

17	COSATI CODES		18 SUBJECT TERMS (Continue on reverse if necessary and identify by block number)
FIELD	GROUP	SUB-GROUP	Surface Enhanced Raman Scattering; electromagnetic and
			chemical mechanisms of enhancement; protonated forms of
			DABCO, selective adsorbtion; application of factor analysis

19 ABSTRACT (Continue on reverse if necessary and identify by block number) to spectra from surfaces.

The Surface Enhanced Raman Spectra of the aliphatic diamine 1,4 diazabicyclo[2.2.2]octane (DABCO) from a silver electrode have been measured as a function of the bulk solution pH. The SER spectrum of the diprotonated DABCO molecule at pH = 1.8 is almost identical to the normal Raman spectrum of the bulk solution at the same pH, in contrast to the SER spectrum of the unprotonated DABCO molecule at pH=12, which shows large differences from the spectrum of the bulk solution at pH = 12. It is proposed that the diprotonated DABCO molecule is co-adsorbed with specifically adsorbed anions, e.g. Cl⁻, and that its spectrum is enhanced by the electromagnetic enhancement mechanism alone. At intermediate pH values, all three possible forms (di, mono and unprotonated) of DABCO are observed, in amounts strongly dependent upon the electrode potential. Both band deconvolution and factor analysis were used to quantify relative populations.

20 DISTRIBUTION/AVAILABILITY OF ABSTRACT ☒ UNCLASSIFIED/UNLIMITED ☐ SAME AS RPT. ☐ DTIC USERS	21. ABSTRACT SECURITY CLASSIFICATION Unclassified	
22a NAME OF RESPONSIBLE INDIVIDUAL Dr. Robert J. Nowak	22b. TELEPHONE (Include Area Code) (519)885-1211 Ext 2500	22c. OFFICE SYMBOL

DD FORM 1473, 84 MAR   83 APR edition may be used until exhausted.
All other editions are obsolete.

The Surface Enhanced Raman Scattering of the Protonated Forms of

DABCO at a Silver Electrode.

David A. Guzonas
Donald E. Irish
George F. Atkinson

Guelph-Waterloo Center for Graduate Work in Chemistry
Waterloo Campus. Department of Chemistry, University of Waterloo,
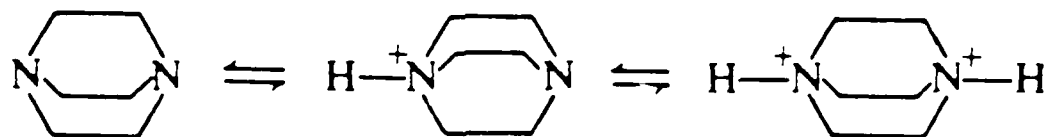Waterloo, Ontario N2L 3G1
Canada

ABSTRACT

The Surface Enhanced Raman Spectra of the aliphatic diamine 1,4 diazabicyclo[2.2.2]octane (DABCO) from a silver electrode have been measured as a function of the bulk solution pH. The SER spectrum of the diprotonated DABCO molecule at pH = 1.8 is almost identical to the normal Raman spectrum of the bulk solution at the same pH, in contrast to the SER spectrum of the unprotonated DABCO molecule at pH=12, which shows large differences from the spectrum of the bulk solution at pH = 12. It is proposed that the diprotonated DABCO molecule is co-adsorbed with specifically adsorbed anions, e.g. Cl^-, and that its spectrum is enhanced by the electromagnetic enhancement mechanism alone. At intermediate pH values, all three possible forms (di, mono and unprotonated) of DABCO are observed, in amounts strongly dependent upon the electrode potential. Both band deconvolution and factor analysis were used to quantify relative populations.

Introduction

The solution pH is an important variable in surface enhanced Raman (SER) studies of electrochemical systems, especially as the adsorbates most frequently studied by SERS are aliphatic or aromatic amines. The importance of pH as an experimental variable can be seen in the studies of the pyridine/silver electrode system. in which the pyridinium ion adsorption was found to be important in understanding the SER spectra (1). In other publications (2.3) we have reported the SER spectra of the diamine 1,4-diazabicyclo[2.2.2.]octane at the pH value of the dilute solution, about pH=12. At this pH DABCO exists almost entirely as the neutral form. with less than 1% existing as the monoprotonated DABCO molecule. The SER spectra of DABCO observed on all substrates studied (silver and gold as both electrodes and colloids) exhibit a striking reduction in the number of bands observed with moderate to strong intensity, compared to the solution spectra. This has led to the proposal that at least part of the surface enhancement for this molecule arises from a photon-driven charge-transfer (PDCT) process such as that proposed by Gersten et al. (4). Ueba (5), Persson (6), and Adrian (7): evidence that such a process plays a role in the SERS of other molecules (e.g.. pyridine) has been presented by Billman and Otto (8), Macomber and Furtak (9). and others. Since DABCO is a diamine and can thus exist in three forms in aqueous solution

$$pK_{a1} = 8.32 \qquad\qquad pK_{a2} = 2.97$$

it was considered important that the SER spectra of the two protonated DABCO

species be studied in some detail. The infrared and Raman spectra of these protonated forms of DABCO have been reported in (10).

There are several a priori reasons for studying these protonated species:

1.   The protonated forms of DABCO are positively charged species, and thus their adsorption behavior on a silver electrode will differ from that of the unprotonated DABCO. Since the diprotonated species is a doubly positively charged species with no lone pairs for bonding with the surface, it would not be expected to be adsorbed on a positively charged electrode;

2.   If the PDCT mechanism proposed for DABCO (2,3) does contribute to the surface enhancement, then the mono-protonation of DABCO might alter the energy levels of DABCO and thus the resonance behavior;

3.   At intermediate pH values (i.e., around pH 6) the distribution diagram shows that all three DABCO species are present in the solution in concentrations which are low for normal solution Raman but which may be significant for the SERS studies. As well, pH values exist at which at least two forms of DABCO are present in solution. It was thus of interest to look for evidence of competitive adsorption;

4.   Differences in the surface pH compared to the bulk solution pH might be expected to manifest themselves in the SERS spectra.

The experimental data to be presented below suggest that all of these effects occur, making interpretation of the spectra obtained at intermediate pH values very difficult. The data at the two pH extremes (very basic and very acidic), where only one of the DABCO species is present in large concentration in the bulk solution, proved to be the easiest to understand. SER spectra obtained from solutions with high pH have already been discussed at great length in previous publications; it was not necessary to consider any of the protonated species in order to understand the SER spectra.

That is. there was no evidence from the SER spectra that at bulk pH values above pH = 10 either of the protonated forms of DABCO adsorbed on the silver electrode The SER spectra obtained from highly acidic solutions (pH less than 2), which are discussed in detail below. are easily understood in terms of the adsorption of the diprotonated DABCO only, although there remain some unresolved mysteries in the data. The SER spectra obtained from solutions of intermediate pH contain numerous bands which show considerable variation with the applied potential. and it appears that at these pH values more than one form of the protonated DABCO can be adsorbed.

Experimental

The electrochemical equipment and the computer interfaced Jarrell-Ash scanning double monochromator have been described in detail in previous publications. A Dilor OMARS-89 spectrometer with optical multichannel analyzer and microscope accessory were also used for part of the work. The OMARS-89 spectrometer was operated using the 1800 groove/mm gratings, with two gratings operating in subtractive mode and a third grating dispersing the output of this stage onto a 512 diode, cooled, diode array detector. The spectrometer was interfaced to an Apple IIe computer for data acquisition: toward the end of the work the Apple IIe was replaced by an IBM AT computer.

The spectra could be transferred to a DEC PRO 380 microcomputer linked to a VAX 11/735. on which an interactive band deconvolution program was available. As well. a factor analysis package (TARGET) obtained from E. R. Malinowski (11) and modified to allow the use of larger (500 x 15) data matrices was available. Two parts of the TARGET package were used in the current work, these being the principal component analysis and key factor spectral isolation programs. The former determines

the number of statistically significant components in a mixture and the latter allows the isolation of the spectra of the pure components, subject to the constraint that there exists for each component one frequency at which that component alone contributes intensity.

DABCO (Aldrich Chem. Co.) was purified by sublimation or by recrystallization from low boiling petroleum ether. All other salts and solvents were reagent grade and used without further purification. All solutions were prepared with distilled deionized water and deoxygenated for one hour prior to use with dry nitrogen. The solution pH was adjusted using concentrated HCl or 3 M perchloric acid, the pH being measured using a Fisher Accumet pH meter.

Silver electrodes were polished using succesive grades of alumina down to 0.3 μm, rinsed and placed in the SERS cell. Roughening was done by a single oxidation-reduction cycle (ORC) unless otherwise stated; the usual ORC was from *-150 to +200* mV and back to -150 mV, at a sweep rate of 20 mV/s, although potential steps with identical limits and 5 to 10 second holding time at the anodic limit were found to give similar results and were sometimes employed. All potentials are given with respect to the saturated calomel electrode (SCE).

Results and Discussion

SERS of the diprotonated DABCO molecule: The SER spectra of the diprotonated DABCO molecule, which will be abbreviated DH_2^{2+}, obtained from a silver electrode potentiostated at -200 mV and at -900 mV, are illustrated in Figure 1 along with the normal Raman spectrum (NRS) of the same species. The solution in the SERS cell was 0.05 M DABCO in 0.1 M KCl, the pH having been adjusted to 1.8 using 12 M HCl. The most striking observation one makes when examining these spectra is the close similarity between the surface spectrum at -200 mV and the NRS

of the diprotonated DABCO molecule: it was the absence of any such similarity between the NRS and SER spectra of the unprotonated DABCO which provided the impetus for the original investigation. In the SER spectrum of DH_2^{2+}, almost all of the bands in the NRS are observed with essentially the same relative intensities. A notable absence is the band at 552 cm^{-1} in the NRS, which is almost undetectable in the SER spectra. The figure also shows that there are substantial changes in the SER spectrum at -900 mV, with new bands appearing in the spectrum. The band frequencies at -300 mV and -600 mV are tabulated in Table 1, along with the band frequencies of the diprotonated DABCO molecule in solution, from reference 10.

At this point one is led to ask, in light of the point made earlier concerning the expected non-adsorption of a doubly positively charged species with no lone pairs on a positively charged electrode surface, how it is possible to obtain a SER spectrum of DH_2^{2+} at -200 mV where the electrode ought to be positively charged? The most plausible hypothesis is that the adsorption of the diprotonated DABCO is made possible by the high concentration of specifically adsorbed chloride ion. The bulk solution was 0.1 M in chloride before the addition of HCl to alter the pH, and therefore the concentration of chloride in the bulk will be much greater than 0.1 M during the SERS experiments. The specific adsorption of a superequivalent amount of chloride would make it possible for the DH_2^{2+} ion to be adsorbed, the adsorption possibly involving a $Cl^- - {}^+HDABCOH^+ - Cl^-$ triple ion, similar to the ion pair proposed for pyridinium ion and chloride (1,12,13,14,15).

A simple experiment to verify this hypothesis was performed by changing the supporting electrolyte to 0.1 M $NaClO_4$ and using $HClO_4$ to alter the solution pH. No SERS of any species could be obtained from this system, even after several ORCs which resulted in an electrode whose surface visually appeared similar to others which

had been found SERS active in perchlorate electrolyte. More work is needed on this aspect of the adsorption of the diprotonated DABCO species, especially involving a comparison between the behavior of the DABCO SERS intensities and the intensity of the Ag-Cl vibration at $240\ cm^{-1}$.

The lack of lone pairs to interact with the electrode surface and the striking similarity of the SER and NR spectra of the diprotonated DABCO molecule stongly suggests that the observed surface enhancement is due only to the electromagnetic (EM) enhancement mechanism. If this is correct, then application of the EM selection rules proposed by Moskovits (16,17) and Creighton (18), should yield information on the orientation of the adsorbed DH_2^{2+} molecule. Assuming the adsorbed molecule, like the molecule in solution, has D_{3h} symmetry, the same results which were obtained for DABCO will apply in this case, viz.,

$$end\text{-}on \qquad a_1{}' > e'' > e'$$

$$edge\text{-}on \qquad a_1{}' > e' > e''$$

for the relative intensities of modes of different species. The application of these rules to the diprotonated species is much easier than for DABCO because modes of all species are observed in the SER spectra. Examination of Table 1 and the spectra in Figure 1 suggests that modes of e'' species are weak or absent (e.g., the absence of ν_{35}), which in turn leads to the conclusion that the diprotonated DABCO molecule is oriented edge-on at the surface, at least at the more anodic potentials. The appearance in the SER spectra of new bands at more negative potentials means that further discussion of the orientation of the molecule must await the identification of these new bands.

Before turning to a discussion of the origins of these new bands, it is useful to pursue the idea that the diprotonated species is enhanced by the EM mechanism only. The SERS intensity, $I_j^i\ (U, \omega_L, \omega_i\ , C_j\ )$ is proportional to the product of four terms,

$$I_j^i (U , \omega_L , \omega_i , C_j) \times \theta_j (U , C_j) \cdot F_{EM}^i (\omega_L , \omega_i) \cdot F_{PDCT}^i (U , \omega_L , \omega_i) \cdot |\bar{E}|^2$$

where U is the electrode potential, $\theta_j (U , C_j)$ is a term which represents the surface concentration of species j and also allows for possible orientation and/or coupling effects. $F_{EM}^i (\omega_L , \omega_i)$ is the enhancement due to the electromagnetic mechanism. $F_{PDCT}^i (U , \omega_L , \omega_i)$ is the enhancement due to the photon-driven charge-transfer mechanism. $\bar{E}$ is the electric field of the incident laser beam. C_j is the bulk concentration of the jth species. ω_L is the excitation frequency and ω_i is the frequency of the Raman shifted photon. In order to illuminate the role played by the term F_{EM} in the overall potential and wavelength behavior of the SERS intensity, the SERS excitation and potential profiles (dependence of the SERS intensity on the excitation wavelength and the electrode potential, respectively) were measured. These should show effects from this term only; this information can then be used to confirm or refute the proposals concerning the existence of a PDCT enhancement mechanism for DABCO. The excitation profile of ν_5 at $\approx 800 \ cm^{-1}$ was measured at two different electrode potentials: the results of duplicate measurements are plotted in Figure 2. All of the points were normalized to the same value at 568.2 nm. The excitation profile for the diprotonated species does not show the potential dependent resonances observed in the excitation profiles for the unprotonated form. although there is a potential-independent maximum near 580 nm and possibly another maximum at wavelengths longer than 650 nm. Neither of these maxima are as large as those measured for DABCO. An examination of the SER spectra of DH_2^{2+} as a function of the electrode potential shows that new bands appear in the spectra as the electrode potential is made more negative. an effect which can be seen more clearly in Figure 3. The most intense of these new features is found at $\approx 1040 \ cm^{-1}$ as a shoulder on the band at 1055 cm^{-1}, the

new band becoming quite strong at -900 mV. Making the electrode potential more negative than this results in the rapid disappearance of the SER spectrum. This can be readily seen in the potential profiles; Figure 4 illustrates the potential profiles for three of the bands of the diprotonated DABCO; a rapid drop in the SERS intensity is apparent at potentials more cathodic than -750 mV. This falloff in the intensity is seen at all excitation wavelengths at the same potential, and the shape of the potential profile is almost independent of the excitation wavelength as well. There are no wavelength-dependent resonance peaks like those found in the potential profiles of DABCO. This is further evidence for the absence of a PDCT enhancement for the diprotonated DABCO molecule.

The potential profiles do show a maximum, however, which at first proved puzzling, but this maximum arises from a shoulder which appears on each of the three bands whose potential profiles were measured. The shoulders on the 997 and 1055 cm^{-1} bands are easily seen in Figure 3, although the shoulder on the 803 cm^{-1} band is not obvious. The appearance of these shoulders in the SER spectra give an increase in the total integrated area measured for the potential profiles, and thus a peak in the potential profile. Because the shoulders are separated from the peak of inter st by up to 10 cm^{-1} they do not fall entirely within the bandpass of the spectrometer, and this may account for the slight differences in the shapes of the potential profiles with changes in the excitation wavelength. The potential profiles of the bands examined in Figure 4 are thus flat until the appearance of the shoulder. To examine the behavior of these new bands in detail, a series of spectra of the 803 cm^{-1} band was deconvoluted, assuming that there were only two component bands beneath the envelope. Several representative spectra, showing the resulting fits, are displayed in Figure 5. The sum of the areas of these two bands reproduces the potential profile of the "803 cm^{-1} band" presented earlier.

Some additional information concerning this species may be obtained from the examination of the cyclic voltammogram of the system. The CV obtained from the same solution and electrode used in a SERS experiment is presented in Figure 6: the effect of hydrogen ion on the CV is apparent, since the onset of hydrogen evolution has shifted to about -700 mV from the value of about -1200 mV in a similar solution at original pH of 10.6. Plotting the cathodic sweep current versus the electrode potential along with the areas of the bands at 798 and 805 cm^{-1} (Figure 7) suggests that there is a correlation between the onset of hydrogen evolution and the appearance of the shoulders in the SER spectra, and that once strong hydrogen evolution is underway, both species are rapidly desorbed.

What then is the identity of this new species? ν_4 and ν_3 are the DABCO bands which show the greatest sensitivity to the environment of the lone pair (2,10). At a potential of -300 mV, ν_4 is found at 1028 cm^{-1}. As the potential is made more negative, this band is replaced by a band at 1034 cm^{-1}, which grows more intense as the potential is made more cathodic. This new band, ν_4 of the new species, is shifted to higher frequency compared to the band at -300 mV, indicative of a stronger lone-pair proton interaction at the more cathodic potentials. One possible model which could account for an increase in the lone pair-proton interaction strength is shown schematically in Figure 8. Part a) of the figure shows a $Cl^- - {}^+HDABCOH^+ - {}^-Cl$ triple ion, which has been proposed in the previous section as possibly existing on the electrode surface at anodic potentials. The protons are thus "shared" with the chloride ions, weakening slightly the lone pair-proton interaction. As the chloride is desorbed, the diprotonated DABCO molecule is hydrated as water replaces the chloride ions. Since the band positions of ν_4 and ν_5 at -600 mV are similar to those of the same bands in the solution spectra of $DABCOH_2^{2+}$, (see Table 1), it is reasonable to assume that

some of the DABCOH_2^{2+} molecules are hydrated at these more cathodic potentials. An alternative hypothesis is that as the chloride ions are desorbed, the molecule "stands up" on the surface, orienting with the N-N axis along the surface normal. Further work is needed to distinguish between these possibilities.

It appears, from this preliminary study of the adsorption of the diprotonated DABCO molecule adsorbed on a silver electrode, that the molecule is adsorbed edge-on, with the N-N axis parallel to the surface, probably in close association with co-adsorbed chloride ions. This species is enhanced by the EM mechanism alone, as evidenced by the relative intensities of the SERS bands, resembling very closely those of the same species in solution, and by the absence of PDCT resonances in the potential and excitation profiles. As the electrode potential is made more negative, a second species appears on the electrode, at potentials at which hydrogen evolution current is observed to begin in the cyclic voltammogram. This new species may be the hydrated, diprotonated DABCO, or the diprotonated DABCO which has reoriented on the surface.

Having now established the appearance of the SER spectrum of the diprotonated DABCO molecule, it is appropriate to turn to the SER spectra at intermediate pH values.

SERS of DABCO at pH 6: It was initially anticipated that the SER spectra at pH 6 would consist only of bands due to the monoprotonated DABCO molecule, since at pH values in this region, the monoprotonated species composes greater than 95% of the bulk DABCO concentration. However, an examination of Figure 9 will quickly convince one that this is not the case, the spectra, especially at the more anodic potentials, containing a large number of bands which appear and disappear with changes in the applied potential. The band frequencies observed at three electrode

potentials are listed in Table 2; it has thus far proven to be impossible to assign every band in the SER spectra at this pH. The spectra clearly become much more simple as the electrode potential is made more negative, the spectra at these more negative potentials appearing very similar to the SER spectra of DABCO in its unprotonated state. The appearance of a shoulder at 1005 cm^{-1}, on the side of the strong band at 985 cm^{-1}, and the appearance of a shoulder at 773 cm^{-1}, on the low frequency side of ν_5 at 793 cm^{-1}, are indicative of the monoprotonated DABCO molecule, these being a_2'' modes in DABCO which become a_1 modes in the monoprotonated species (cf., Table 2 of Ref. 10). The band at 1035 cm^{-1} is highly suggestive of the diprotonated species, since there is no band at this frequency for either the mono- or unprotonated DABCO. A comparison of the band positions in Table 2 and Table 1 suggests that at the most anodic potentials, the diprotonated and the monoprotonated DABCO molecules are both adsorbed on the electrode surface; as for the diprotonated form, the adsorption of the monoprotonated DABCO at a positively charged electrode is reasonable only if the adsorbed DH^+ is coadsorbed with chloride ions. As the potential is made more negative, the diprotonated form is desorbed, since the band at, for example, 1035 cm^{-1} has disappeared at a potential of -400 mV.

Interesting changes are seen to occur in the 600 cm^{-1} region over the entire potential range studied. At the most anodic potentials, bands at 603 and 651 cm^{-1} are observed; as the electrode potential is made more negative, a new band at 626 cm^{-1} appears in the spectrum, the band at 651 cm^{-1} disappearing at more negative potentials. The identity of the 651 cm^{-1} band, which was also seen in the SER spectra of the diprotonated DABCO presented in the previous section, is not known, but its presence in the spectra of the diprotonated DABCO at pH 1.8, and in the spectra at pH 6 discussed here, suggests that it is associated with the diprotonated DABCO.

The band at 603 cm^{-1} is then assigned to the monoprotonated DABCO, and the band at 626 cm^{-1} to the unprotonated DABCO (this band, ν_6, is found at 617 cm^{-1} in the SER spectra of DABCO at pH 10.6).

Another band with unusual behavior is found at 1349 cm^{-1}, the band showing a rapid rise in intensity at potentials between -400 and -550 mV; at more cathodic potentials, all of the SERS bands become weaker in intensity. This band is clearly ν_3, and it must be ν_3 of the *unprotonated* DABCO because this band is found at 1364 cm^{-1} in the monoprotonated DABCO; a band at 1363 cm^{-1} is observed at potentials more anodic than -400 mV. This observation, along with the presence of a band at 626 cm^{-1} suggests that at the more cathodic potentials, both the mono- and unprotonated DABCO molecules are adsorbed on the electrode.

It appears from the SER spectra at pH 6 that all three protonated forms of DABCO are adsorbed on the silver electrode at pH 6, the identity of the species depending upon the electrode potential, and probably on the presence or absence of adsorbed chloride. A more detailed discussion of the SER spectra, such as an assignment of all of the adsorbed bands, will have to await further experiments. One such experiment involved examination of the SER spectra at a pH intermediate of pH = 1.8 and pH = 6.0; the pH chosen was pH = 4.5, and these experiments are the subject of the next section.

The SERS of DABCO at pH 4.5: At pH 4.5, the DABCO distribution diagram shows that the monoprotonated species comprises greater than 95% of the total concentration in the bulk solution, the remainder being the diprotonated form. At this pH the SER spectrum was therefore expected to contain contributions from only two species, presenting a much less complex mixture than the spectra obtained at pH 6.

Three spectral regions were studied in detail, these being 550-850, 950-1100 and 1300-1400 cm^{-1}, as illustrated in Figure 10, Figure 11 and Figure 12 respectively. As in the pH 6 spectra, a number of new bands are seen to appear in the pH 4.5 spectra as the electrode potential is made more negative, most notably a shoulder at 616 cm^{-1}, a band at 990 cm^{-1}, and a band at 1350 cm^{-1}; the first and last bands mentioned appear and disappear over a very narrow (300 mV) potential range; this behavior is similar to the behavior of bands at the same positions in the pH = 6.0 spectra. These spectra are, however, less congested at the more anodic potentials than were the pH = 6.0 spectra, making an assignment more feasible. In order to identify the species present and attempt to quantify the changes in the spectra, the spectra were deconvoluted. Good fits to the band contour could be obtained with only two component bands, one at 603 cm^{-1} and the other at 618 cm^{-1}; a weaker band at 559 cm^{-1} was present in some of the spectra. Interestingly, the band at 651 cm^{-1} observed in the SER spectra obtained at pH = 6.0 and pH = 1.8 is not observed in the pH = 4.5 spectra, adding to the mystery concerning the identity of this band.

The strong band at about 800 cm^{-1} was also deconvoluted, but considerable difficulty was encountered in deciding upon the number of component bands present, because of close overlap. It appears that two closely overlapping bands are probably present, separated by only about 2 cm^{-1}, which is not surprising since this band rarely exhibits a large frequency shift with either electrode potential or pH (10).

The spectral region from 950-1000 cm^{-1} contains a large number of bands at positive potentials, six component bands being needed to give a good fit as shown in Figure 13. At the most positive potential, bands are found at 975, 992, 1006, 1024, 1044, and 1055 cm^{-1}. As the potential is made more negative (e.g., -500 mV), the spectrum becomes dominated by bands at circa 990 and 1007 cm^{-1} with weaker bands at 1050 and 975 cm^{-1}, the latter a shoulder. At still more negative potentials, the

shoulder at 975 cm^{-1} becomes more intense; finally the intensity rapidly decreases until at potentials cathodic of -800 mV the spectrum becomes essentially undetectable. At these more negative potentials, only four component bands were required to give a good fit.

In the 1300-1500 cm^{-1} region there are again a large number of component bands necessary to give a good fit at the more positive potentials. Like the spectra in the 950-1100 cm^{-1} region, the spectra are weak at the positive potentials, and were also found to exhibit oddly sloping baselines which were very difficult to remove; these baselines arose in part from the presence of a number of broad, overlapping bands near 1300 cm^{-1}. However, in spite of these difficulties, good fits could be obtained. Because of baseline problems, difficulties were encountered with some of the areas, especially at the more positive potentials; this only affected the weak bands at these potentials. A band at 1350 cm^{-1} is seen to undergo a large variation in intensity over a narrow range of potentials, as mentioned earlier and many other bands are observed to exhibit intensity changes.

Since all three spectral regions contain bands which exhibit a strong variation in intensity over a narrow potential range, it was suspected that these bands arise from the same species, yet to be identified. The band areas from the curve resolution are thus plotted versus the electrode potential in Figure 14 a), b) and c) for the three regions 550-700, 959-1100 and 1300-1500 cm^{-1} respectively. The plot suggests that there are three distinct species whose intensities exhibit very different behavior with changes in the applied potential; these species have been labelled I, II, and III in the figure. The bands attributed to these species are listed in Table 3, and a comparison of the band positions in this table with those listed in Tables 1 and 2 allows the three species to be identified as diprotonated DABCO (species I), monoprotonated DABCO (species II) and DABCO (species III).

As a further check on the results described above obtained by deconvolution of the SER spectra, the spectra in the 950-1100 cm^{-1} range were analysed using the factor analysis package. The principal component analysis indicated that three components were present in these spectra; the key factor spectral isolation program was then used to produce the spectra of these three species (Figure 15). The spectra of the three isolated components are essentially identical to those inferred from the curve resolution analysis; the negative peak in the spectrum of the first component arises because of the severe band overlap in this region, making it difficult for the program to find a unique frequency for each component at which it alone scatters. The spectrum of the monoprotonated DABCO species is similar to the spectrum of this species inferred at pH = 6.0. The relative intensities of these species as obtained from the spectral isolation program are plotted in Figure 16. Comparing this plot with that obtained using the curve resolution data suggests the correctness of the curve resolution procedure, and also illustrates the possible utility of factor analysis in SERS.

The plots of intensity versus electrode potential can be interpreted in the following way. Since the diprotonated DABCO species has been shown to be enhanced by the EM mechanism only, the intensity drop exhibited by the bands assigned to this species indicate that it is being desorbed as the electrode potential is made more negative. This is in accord with the argument presented in the previous section where it was suggested that chloride ion must be present in order to have adsorption of the diprotonated form; as the electrode is made more negative, chloride is desorbed, thus desorbing the $DABCOH_2^{2+}$. The presence of this species at the electrode is somewhat surprising at this pH, since it forms only 5% of the total concentration of DABCO species in the bulk solution, suggesting that at positive potentials in the presence of chloride this species is preferentially adsorbed, possibly due to a difference between the surface and bulk pH's and/or the greater stability of the triple ion. Sun et al. (15),

in their SERS study of the adsorption of pyridinium ion at silver electrodes, observed a decrease in the surface pH due to a shift in the electrostatic potential at the outer Helmholtz plane caused by the specific adsorption of chloride ion; such an effect would also explain the results reported here.

At the same time that the intensities of the $DABCOH_2^{2+}$ bands are decreasing, the bands assigned to $DABCOH^+$ are seen to increase in intensity; unfortunately, it is difficult to decide whether this increase results from a change in the population of this species or results from a PDCT resonance as found for DABCO. The appearance of the spectra is suggestive of a charge transfer complex, since the spectrum is dominated by ν_4, ν_5, and ν_8 as in the SER spectra of DABCO. Interestingly, ν_3 is not seen to be enhanced in the SER spectrum of the monoprotonated species. The absence of this band suggests that the protonation of DABCO perturbs the electron distribution in the molecule sufficiently to "unmix" the totally symmetric C-C stretching and C-H wagging normal coordinates (2). Further evidence could be obtained from the potential profiles; however these would have to be obtained by scanning discrete spectra at 50 mV intervals, curve resolving the spectra and then plotting out the potential profile, because of the severe band overlap. This process would have to be repeated at each excitation wavelength. It can be concluded, however, that the rapid decrease in intensity at potentials more cathodic than -700 mV is a result of desorption, rather than the SERS mechanism.

The same difficulty arises in interpreting the meaning of the intensity changes observed for the DABCO bands, which are seen to rise and fall in intensity over a potential range of only about 300 mV. However, the shape and position of the PDCT resonance for these bands are known from previous work (2,3). The potential profiles ascribed to the PDCT resonance in DABCO are considerably wider (full width at half maximum=350 mV) than the intensity peaks seen in the pH 4.5 plots, these

having a full width at half maximum of 160 mV. These intensity variations at pH 4.5 must therefore be due mainly to changes in the concentration of DABCO at the electrode surface. The observation of bands due to DABCO at this pH is very surprising, since the bulk solution contains less than 1 % of the unprotonated DABCO. This suggests that there is some interesting chemistry taking place at the surface in this system, involving an apparent change in the surface pH.

Finally, it was possible to monitor the surface equilibrium of the three DABCO species as a function of the bulk pH, by doing an in-situ 'titration' of the bulk solution. Starting with a SERS active surface obtained as described earlier, with a bulk solution containing 0.1 M KCL, and 0.05 M DABCO at pH 1.8, the multichannel detector was set for a 0.2 s aquisition time, the result of each aquisition being displayed on the computer. Sufficient 50% NaOH to make the entire solution in the SERS cell pH=12 was rapidly injected into the cell with a syringe placed close to the electrode, while the video sceen was monitored. The SER spectrum was observed to rapidly pass from that of the diprotonated DABCO, through that of the monoprotonated form, and finally ending with the spectrum of the neutral DABCO molecule (Fig. 17). The process was completely reversable when acid was added to the pH=12 solution.

Conclusions

Diprotonated DABCO adsorbs on a silver electrode surface at potentials positive of the point of zero charge, facilitated by halide ion. The EM theory of the surface enhancement adequately accounts for the appearance of the SER spectra. At pH values where $DABCOH_2^{2+}$ is a minor species, it is still observed at positive potentials and appears to be preferentially adsorbed over the monoprotonated species. This may point

up the existence of a surface pH lower than that of the bulk solution or the greater affinity of this former species for chloride ion. For the first time factor analysis has been applied to SER spectra to identify and quantify the surface species. Also. the conversion of surface species from protonated to unprotonated forms (and the reverse) has been visually monitored spectroscopically in- situ. At intermediate pH values all three forms of DABCO have been detected on the surface. The spectra of the mono-protonated form suggets that. like DABCO itself. the PDCT mechanism provides part of the surface enhancement.

Acknowledgements

REFERENCES

1.   Rogers, D. J.; Luck, S. D.; Irish, D. E.; Guzonas, D. A.; Atkinson, G.F. J. Electroanal. Chem. 1984, 167, 237.

2.   Irish, D. E.; Guzonas, D. A.; Atkinson, G. F. Surf. Sci. 1985, 158, 314.

3.   Guzonas, D. A.; Irish, D. E.; Atkinson, G. F. submitted

4.   Gersten, J. I.; Birke, R. L.; Lombardi, J. R. Phys. Rev. Lett. 1979, 43, 147.

5.   Ueba, H. J. Chem. Phys. 1980, 73, 725.

6.   Persson, B. N. J. Chem. Phys. Lett. 1981, 82, 561.

7.   Adrian, F. J. J. Chem. Phys. 1982, 77, 5302.

8.   Billman, J.; Otto, A. Solid State Comm. 1982, 44, 105.

9.   Macomber, S. H.; Furtak, T. E. Surf. Sci. 1982, 122, 556.

10.   Guzonas, D. A.; Irish, D. E. Can. J. Chem. 1988, 66, 1249.

11.   Malinowski, E. R. Target 85 Programs, Lake Hiawatha, N. J., 1985.

12.   Regis, A.; Corset, J. Chem. Phys. Lett. 1980, 70, 305.

13.   Atkinson, G. F.; Guzonas, D. A.; Irish, D. E. Chem. Phys. Lett. 1980, 75, 557.

14.   Birke, R. L.; Bernard, I.; Sanchez, L. A.; Lombardi, J. R. J. Electroanal. Chem. 1983, 150, 447.

15.   Sun, S. C.; Bernard, I.; Birke, R. L.; Lombardi, J. R. J. Electroanal. Chem. 1985, 196, 359.

16.   Moskovits, M.; Suh, J. S. J. Phys. Chem. 1984, 88, 5526.

17.   Moskovits, M. Rev. Mod. Phys. 1985, 57, 783.

18.   Creighton, J. A. Surf. Sci. 1985, 158, 211.

FIGURE CAPTIONS

Figure 1. The SER spectra (upper two spectra) and normal Raman spectrum (lower) of the diprotonated DABCO molecule.

Figure 2. SERS excitation profiles for the diprotonated DABCO molecule adsorbed on a silver electrode, measured at -200 and -600 mV vs SCE.

Figure 3. The SER spectra of diprotonated DABCO on silver as a function of the electrode potential. The excitation wavelength was 514.5 nm.

Figure 4. Potential profiles of three bands of the diprotonated DABCO molecule, excited using the 568.2 nm krypton laser line. The lower trace shows the potential profile of the 805 cm^{-1} band obtained using 647.1 nm excitation.

Figure 5. The goodness of fit of the curve resolution of the CN stretching mode of diprotonated DABCO adsorbed on a silver electrode.

Figure 6. Cyclic voltammogram (CV) of a silver electrode in 0.1 M KCl, 0.05 M DABCO at pH= 1.8, using a sweep rate of 20 mV/s.

Figure 7. Plot of the cathodic current from Figure 6 and the band areas of the 800 and 807 cm^{-1} bands versus the electrode potential.

Figure 8. A model for the two diprotonated DABCO species found at cathodic potentials. In a), the $Cl^- - {}^+HDABCOH^+ - Cl^-$ ion pair is adsorbed at a positively charged electrode. In b), the chloride ions have been desorbed and replaced by water.

Figure 9. Dependence of the SER spectra of DABCO at pH = 6.0 on the electrode potential. The solution contained 0.1 M KCl, 0.05 M DABCO. The excitation wavelength was 568.2 nm. The electrode potential is given on the right hand side of each spectrum.

Figure 10. The CN stretch and cage deformation region of the DABCO SER spectra at pH 4.5.

Figure 11. The CC stretching region of the DABCO SER spectra at pH 4.5.

Figure 12. The CH wag and scissors region of the DABCO SER spectra at pH 4.5.

Figure 13. The goodness of fit for the CC stretching region at pH 4.5.

Figure 14. The integrated areas versus the electrode potential for bands in the spectral regions a) 550-700, b) 950-1100, and c) /1300-1500 cm^{-1} . The labels I, II and III are explained in the text.

Figure 15. The Raman spectra of the three component species at pH 4.5 as obtained from the spectral isolation program. The lower spectrum corresponds to species 1, the centre to species II, and the upper spectrum to species III.

Figure 16. The relative concentrations of species I, II and III versus the electrode potential, as determined by factor analysis of the spectra of the 950-1100 cm^{-1} region.

Figure 17. The SER spectra of DABCO and diprotonated DABCO obtained from the same electrode in an in-situ 'titration' experiment. The upper spectrum was recorded at pH=1.8, the lower spectrum after the addition of base.

Table 1: Band positions of diprotonated DABCO SERS bands.

Band Frequency cm^{-1}			Assignment
-300 mV	-600 mV	solution	
407	406	404	ν_{27}
---	437	---	---
---	463	---	?
---	558	---	ν_{35}
605	602	605	ν_8
648	---	---	?
803	803	809	ν_5
---	819	---	?
898	886	903	ν_{25}
980	987	987	ν_{34}
----	1008	----	ν_{16} ?
1028	1034	1033	ν_4
1057	1045	1061	ν_{24}
1163	1145	----	?
----	1201	----	?
1282	1280	----	?
1282,br	1282,br	1280,br	NH^+ bend
1318	1309	1299	ν_{23}
1397	1411	1407	ν_3
1448	1442	1443	ν_{30}
1464	1455	1476	ν_{21}

    --- not observed
     ? no assignment possible

Table 2: The band frequencies of DABCO adsorbed on silver at pH = 6.0

Electrode Potential

-150 mV	-400 mV	-600 mV
603 m	607 ms	613 ms
---	626 ms	620 ms
651 mw	645 ms 646 w.sh	
758 w	752 w	---
---	---	778 w.sh
801 vs	794 s	793 ms
894 mw	---	---
946 mw	940 w	---
998 vs	986 vs	985 s
1012 m.sh	1007 m.sh	1005 w.sh
1035 m.sh	---	---
1055 m	1048 w	---
1087 mw	---	---
1109 w	1122 w	---
1164 mw	1154 w	---
1226 w	1214 w	1236 w
---	1236 w	---
---	1292 w	---
1322	1315 w	---
1355 ms	1349 vs	1344 s
1363 ms	---	---
1415 mw	---	---
1435 mw,sh	1442 w.sh	---
1466 ms	1460 mw	1458 mw
1514 mw,sh	1515 w	---
1527 m	---	---
---	1588	---
1622	1610	---

w   weak
m   medium
s   strong
v   very
sh shoulder
-- not observed

band frequencies are given in cm^{-1}

Table 3: Band frequencies of bands assigned to the three species observed

Species I	Species II	Species III	Assignment
	560		ν_{35}
?	603	619	ν_{6}
?	803	?	ν_{5}
	840		ν_{28}
1024	992	979	ν_{4}
	1006		ν_{17}
1055	1044	?	ν_{24}
	1300		ν_{23}
	1316?		?
1390	1363	1348	ν_{3}
	1381		ν_{16}
	1458?	1438?	ν_{30}
1498	1480	1458	ν_{2}

Band frequencies are in cm^{-1}
? denotes uncertainty in the assignment

re 1. The SER spectra (upper two spectra) and normal Raman spectrum (lower) of the diprotonated DABCO molecule.

Figure 2. SERS excitation profiles for the diprotonated DABCO molecule adsorbed on a silver electrode, measured at -200 and -600 mV vs SCE.

Figure 3. The SER spectra of diprotonated DABCO on silver as a function of the electrode potential. The excitation wavelength was 514.5 nm.

Figure 4. Potential profiles of three bands of the diprotonated DABCO molecule, excited using the 568.2 nm krypton laser line. The lower trace shows the potential profile of the 805 cm^{-1} band obtained using 647.1 nm excitation.

Figure 5. The goodness of fit of the curve resolution of the CN stretching mode of diprotonated DABCO adsorbed on a silver electrode.

Figure 6. Cyclic voltammogram (CV) of a silver electrode in 0.1 M KCl. 0.05 M DABCO at pH= 1.8. using a sweep rate of 20 mV/s.

Figure 7. Plot of the cathodic current from Figure 6 and the band areas of the 800 and 807 cm^{-1} bands versus the electrode potential.

Figure 8. A model for the two diprotonated DABCO species found at cathodic potentials. In a), the $Cl^- - {}^+HDABCOH^+ - Cl^-$ ion pair is adsorbed at a positively charged electrode. In b), the chloride ions have been desorbed and replaced by water.

Figure 9. Dependence of the SER spectra of DABCO at pH = 6.0 on the electrode potential. The solution contained 0.1 M KCl. 0.0 M DABCO. The excitation wavelength was 568.2 nm. The electrode potential is given on the right hand side of each spectrum.

Figure 10. The CN stretch and cage deformation region of the DABCO SER spectra at pH 4.5.
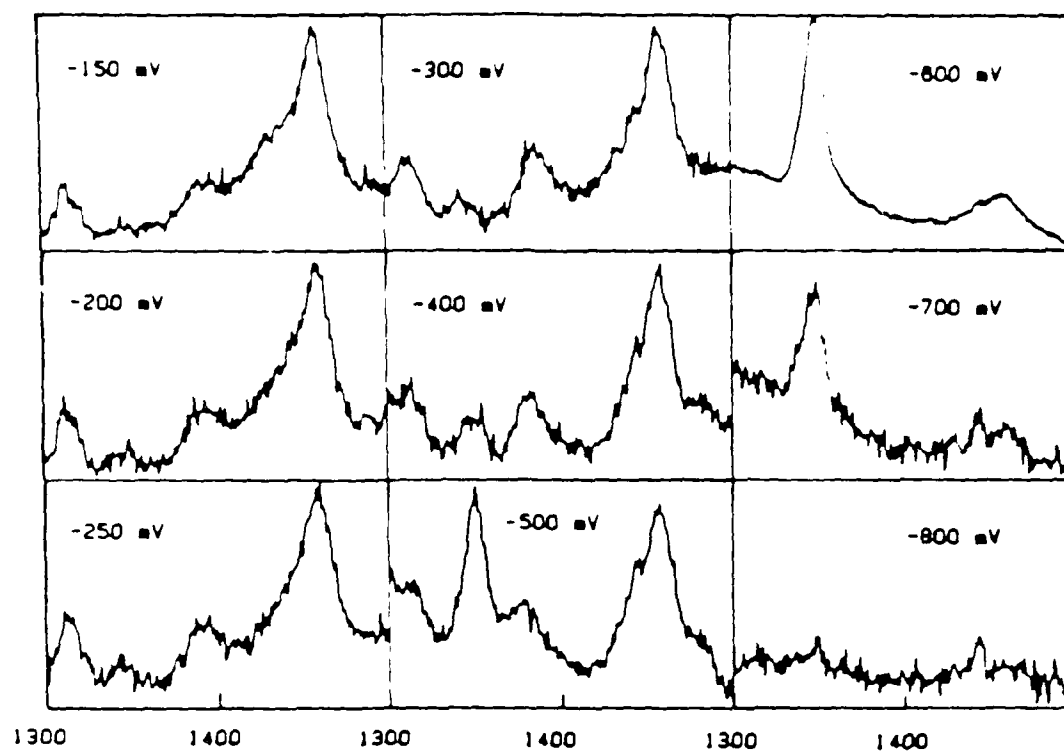
Raman shift / cm^{-1}

Figure 11. The CC stretching region of the DABCO SER spectra at pH 4.5.

Raman shift / cm^{-1}

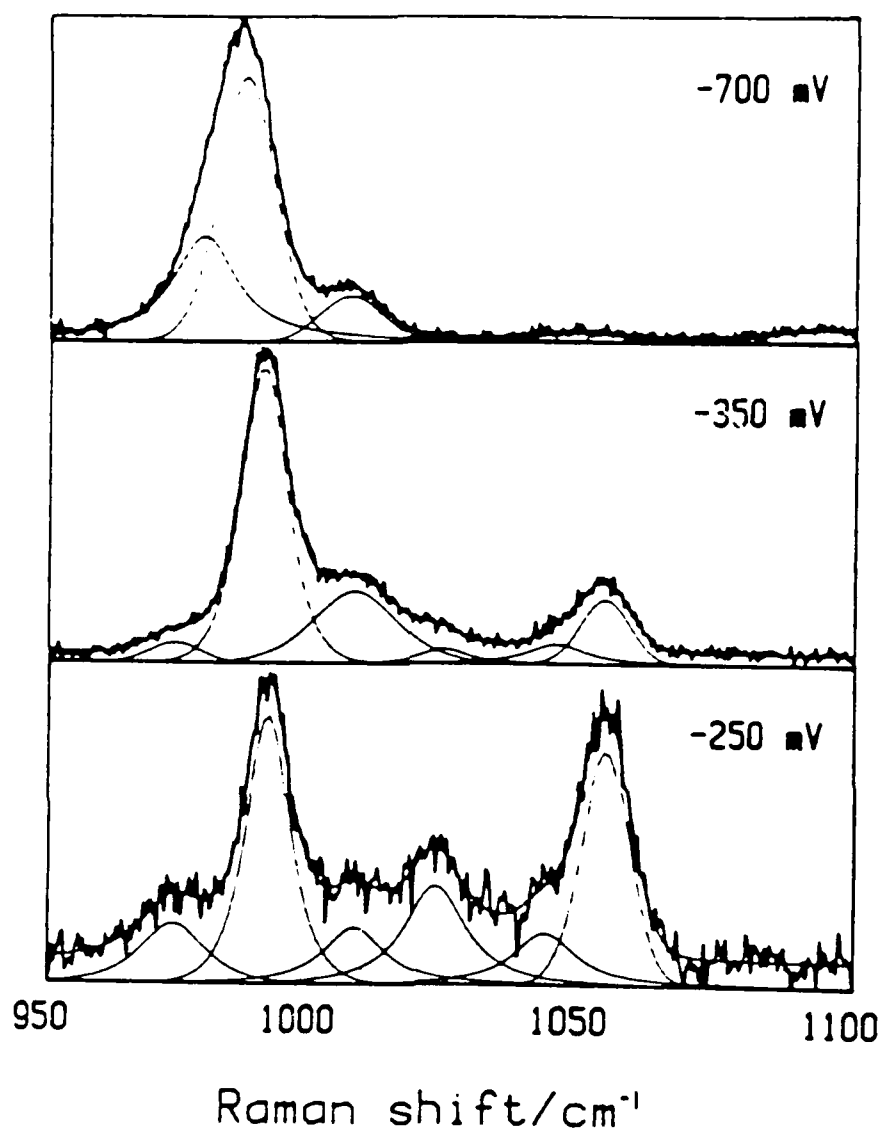Figure 12. The CH wag and scissors region of the DABCO SER spectra at pH 4.5.

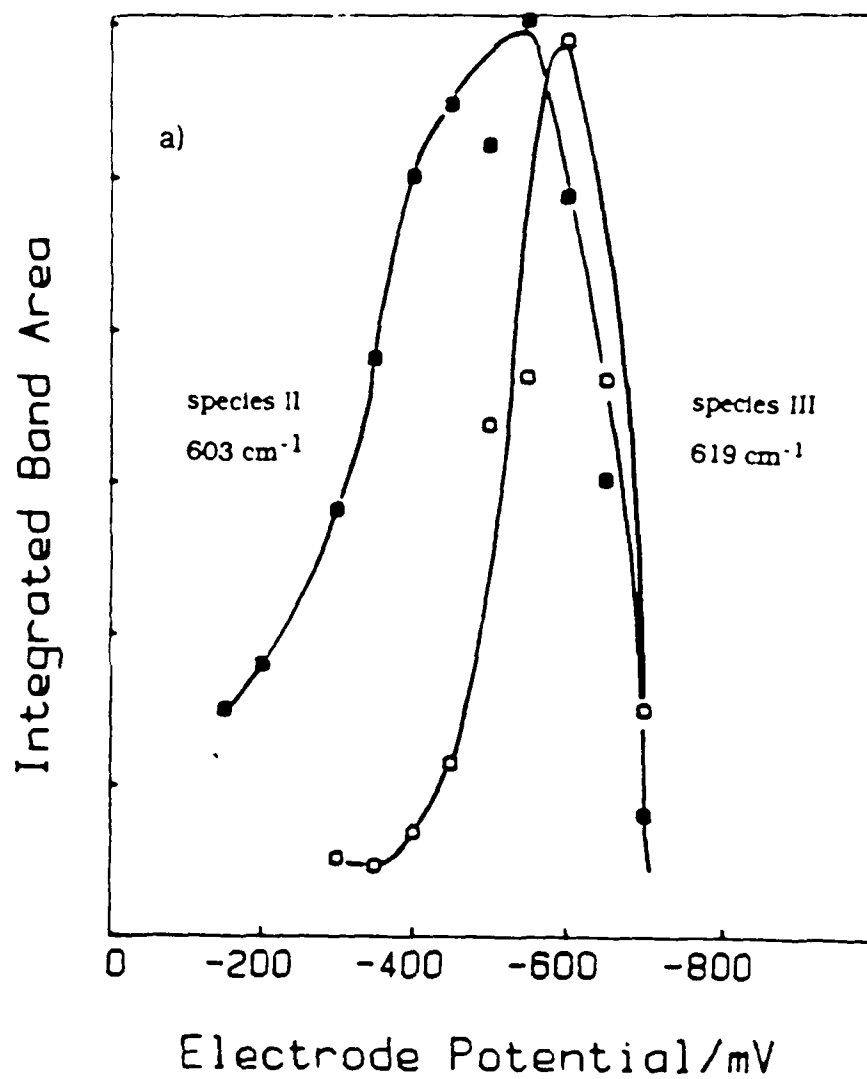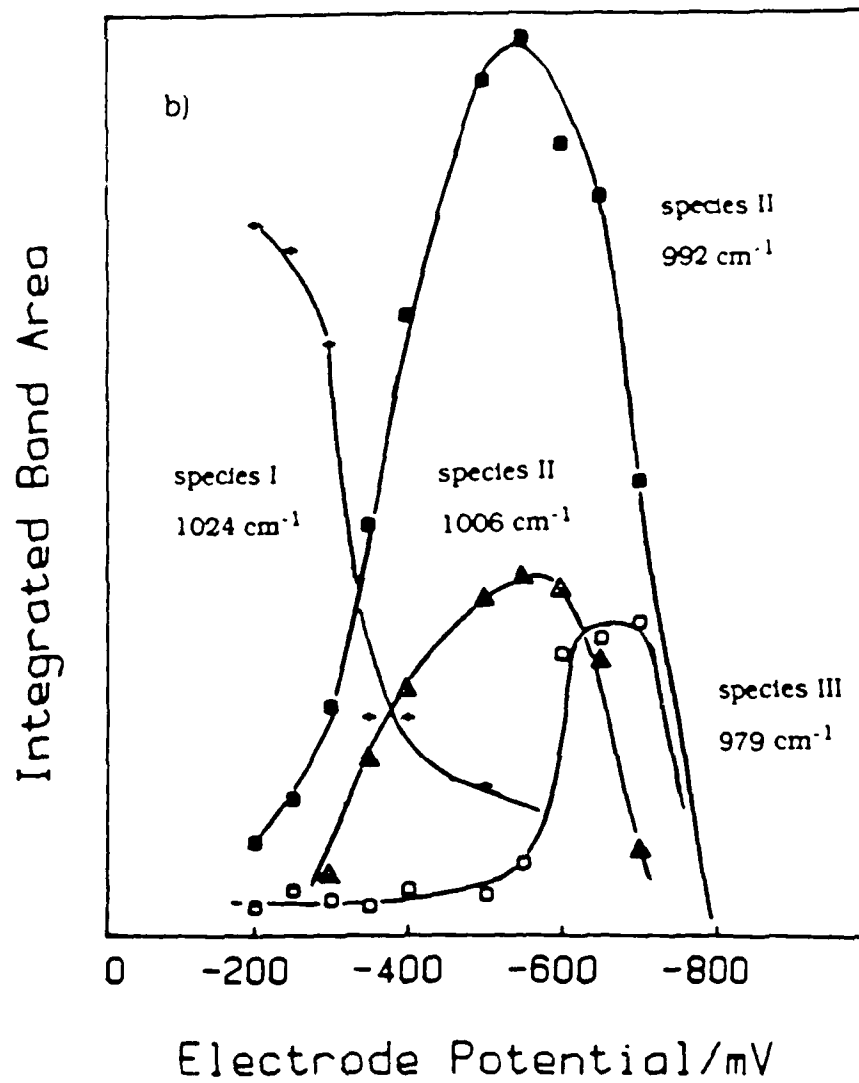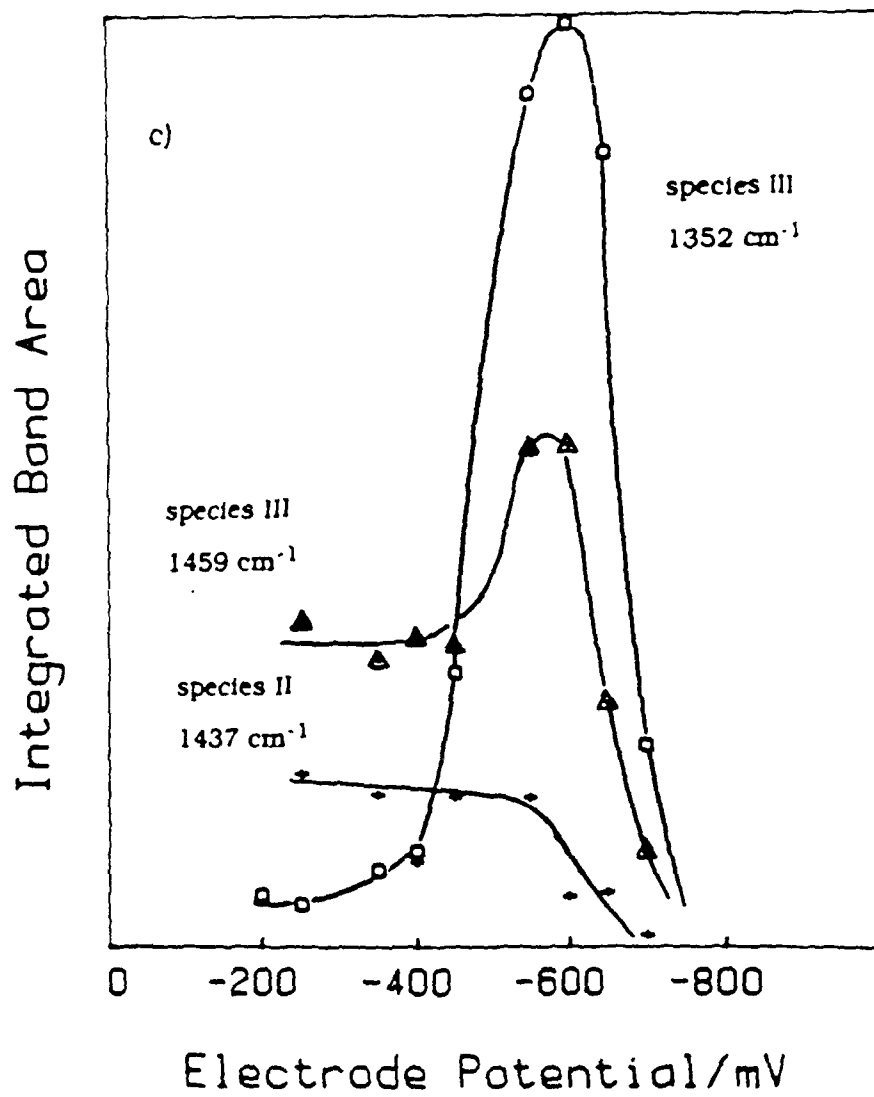Figure 13. The goodness of fit for the CC stretching region at pH 4.5.

Figure 14. The integrated areas versus the electrode potential for bands in the spectral regions a) 550-700. b) 950-1100. and c) /1300-1500 cm^{-1}. The labels I. II and III are explained in the text.

b)

species II
992 cm^{-1}

species I   species II
1024 cm^{-1} 1006 cm^{-1}

species III
979 cm^{-1}

Integrated Band Area

Electrode Potential/mV

0   -200   -400   -600   -800

14.b.

c)

Integrated Band Area

species III
1352 cm^{-1}

species III
1459 cm^{-1}

species II
1437 cm^{-1}

Electrode Potential/mV
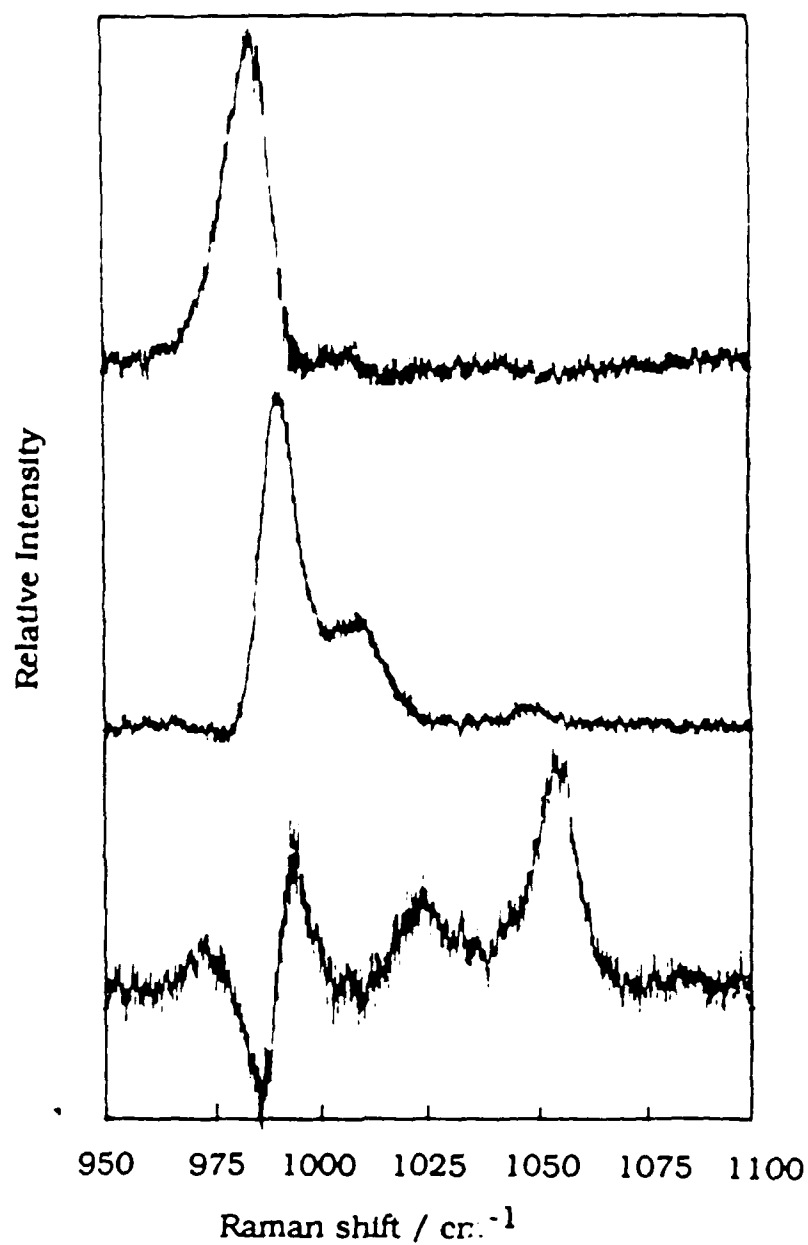
0   -200   -400   -600   -800

14 c)

Figure 15. The Raman spectra of the three component species at pH 4.5 as obtained from the spectral isolation program. The lower spectrum corresponds to species I. the centre to species II. and the upper spectrum to species III.
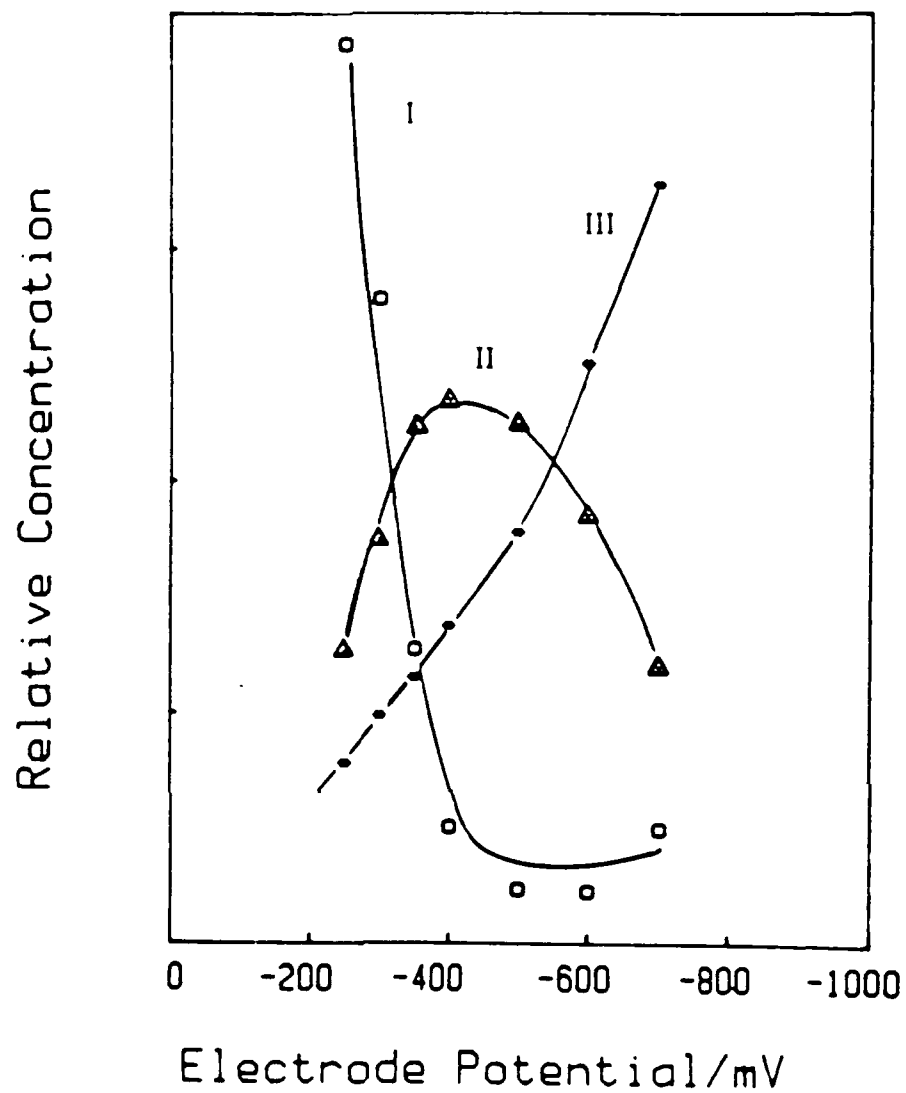
Figure 16. The relative concentrations of species I, II and III versus the electrode potential, as determined by factor analysis of the spectra of the 950-1100 cm^{-1} region.
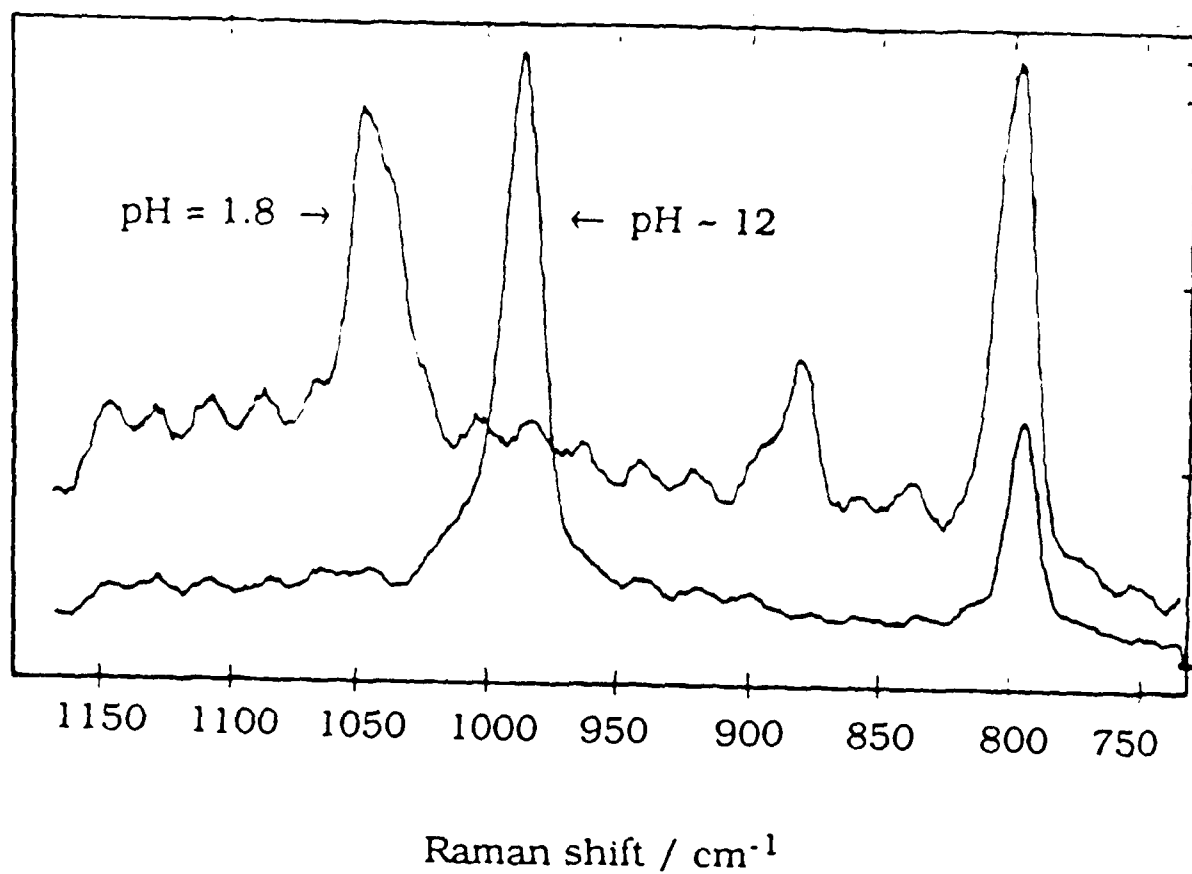
pH = 1.8 →   ← pH ~ 12

Raman shift / cm⁻¹

Figure 17. The SER spectra of DABCO and diprotonated DABCO obtained from the same electrode in an in-situ 'titration' experiment. The upper spectrum was recorded at pH=1.8, the lower spectrum after the addition of base.

TECHNICAL REPORT DISTRIBUTION LIST, GEN

	No. Copies		No. Copies
Office of Naval Research Attn: Code 1113 800 N. Quincy Street Arlington, Virginia 22217-5000	2	Dr. David Young Code 334 NORDA NSTL, Mississippi 39529	1
Dr. Bernard Douda Naval Weapons Support Center Code 50C Crane, Indiana 47522-5050	1	Naval Weapons Center Attn: Dr. Ron Atkins Chemistry Division China Lake, California 93555	1
Naval Civil Engineering Laboratory Attn: Dr. R. W. Drisko, Code L52 Port Hueneme, California 93401	1	Scientific Advisor Commandant of the Marine Corps Code RD-1 Washington, D.C. 20380	1
Defense Technical Information Center Building 5, Cameron Station Alexandria, Virginia 22314	12 high quality	U.S. Army Research Office Attn: CRD-AA-IP P.O. Box 12211 Research Triangle Park, NC 27709	1
DTNSRDC Attn: Dr. H. Singerman Applied Chemistry Division Annapolis, Maryland 21401	1	Mr. John Boyle Materials Branch Naval Ship Engineering Center Philadelphia, Pennsylvania 19112	1
Dr. William Tolles Superintendent Chemistry Division, Code 6100 Naval Research Laboratory Washington, D.C. 20375-5000	1	Naval Ocean Systems Center Attn: Dr. S. Yamamoto Marine Sciences Division San Diego, California 91232	1

24